

Stopping power for swift dressed ions

C. C. Montanari* and J. E. Miraglia

Instituto de Astronomía y Física del Espacio, Consejo Nacional de Investigaciones Científicas y Técnicas and Departamento de Física, Facultad de Ciencias Exactas y Naturales, Universidad de Buenos Aires, Casilla de Correo 67, Sucursal 28, (C1428EGA) Buenos Aires, Argentina

(Received 22 March 2005; published 9 February 2006; corrected 3 March 2006)

We present theoretical calculations of electronic stopping power, including excitation and loss of both projectile and target electrons. The energy loss due to target valence and inner-shell electrons are separately evaluated: the former in the usual dielectric formalism, and the latter by employing a shell-wise local plasma approximation. Stopping power calculations of He ions in Al and Zn are presented, including the electron-electron contribution mentioned above. The agreement with the experimental data is very good, and let us conclude that, for helium ions, projectile excitation and loss contribute to the stopping power at the most in 1%, and it is reasonable for the theoretical descriptions to neglect it.

DOI: [10.1103/PhysRevA.73.024901](https://doi.org/10.1103/PhysRevA.73.024901)

PACS number(s): 34.50.Bw, 34.50.Fa, 71.10.-w, 71.45.Gm

The stopping power for ion-matter collisions is related to the electronic structure and dynamics of the atoms, molecules, or crystals involved. From the early work of Bohr [1], the quantum-mechanical treatment of Bethe and Bloch [2,3], and the many-body development of Lindhard [4], the theoretical approaches to calculating the energy loss of light and heavy particles in matter can be separated into two main lines: the binary collisional formalism (charged particle stopping is treated as a sequence of binary collisions) and the dielectric formalism (target electrons are supposed to respond to the ion passage as a gas of free electrons).

In the last two decades, great advances were made within the binary collisional formalism [5–9], towards the description of the low- and intermediate-energy regime where Bethe theory does not apply [10]. The theoretical basis for the dielectric formalism was developed during the 1950s and 1960s [4,11–14]. It is based on the original work by Lindhard [4] who proposed a many-body consistent treatment for the response of an electron gas to the ion perturbation, within the linear response approximation [15]. This model may be used to describe not only metal valence electrons, but also inner-shell ones, by treating bound electrons as an inhomogeneous free electron gas [11,14]. This approach is usually referred to as local plasma approximation (LPA). The LPA was extended to isolated Hartree-Fock atoms by Chu and co-workers [16] and to solids by Ziegler [17].

Different expressions for the stopping power have been proposed within the approach of a local density of free electrons [18–20]. In the present contribution we employ a shell-wise local plasma approximation (SLPA). We have already used this SLPA in previous studies in which we obtained a very good description of the experimental data for energy loss, straggling, and ionization cross sections in different gaseous and solid targets [21–25].

This work deals with electronic stopping power for neutral ions colliding with a metallic bulk. These ions arrive to an equilibrium charge state within the solid that will be neu-

tral, partially stripped, or bare, depending on the ion velocity. Usually, stopping power calculations in the intermediate- to high-energy range, only consider the interaction of target electrons with the projectile nucleus, partially screened by its bound electrons. However, target electrons interact both with the partially screened nucleus (screening mode), and with the projectile electrons (antiscreening mode) [26]. In fact, the inelastic transitions of projectile electrons (excitation, loss, capture) are responsible for the different charge states of the ion inside the solid.

The aim of this work is to present stopping power calculations, including the antiscreening mode, and to analyze the importance of this contribution. We make a detailed calculation that separately considers the contributions of inner-shell and valence electrons. The stopping power of He ions on Al and Zn is compared with the experimental data available in the literature showing very good agreement.

When a fast heavy ion moves in a medium, it polarizes the target electron cloud. This gives rise to an induced potential [27], which can be described as a trailing wake that follows the motion of the projectile (dynamic screening) [27–29]. Following Lindhard dielectric formalism [4,11], the retarding force or stopping power per unit length on a bare ion is expressed as

$$S = \frac{2Z_p^2}{\pi v^2} \int_0^\infty \frac{dk}{k} \int_0^{kv} \omega \operatorname{Im} \left[\frac{-1}{\varepsilon(k, \omega)} \right] d\omega, \quad (1)$$

with Z_p and v being, respectively, the charge and velocity of the impact ion, and $\varepsilon(k, \omega)$ the dielectric function of the medium.

In the case of metals, electrons are treated differently depending on whether they belong to the free electron gas (FEG), or to the inner shells. For the FEG, we use the Mermin dielectric function [30] to account for the plasmon time decay. This dielectric function depends on the constant density of electrons ρ_{FEG} and satisfies the f -sum rule. For target inner shells we employ the LPA, and the approximation of independent shell response. We employ the SLPA notation to underline this difference with the usual LPA. Considering the electron density of the nl shell $\rho_{nl}(r)$, its local dielectric re-

*Electronic address: mclaudia@iafe.uba.ar

sponse is given by $\varepsilon[k, \omega, \rho_{nl}(r)]$. The energy loss function in the SLPA is obtained as a mean spatial value of the local one [20,22]

$$\text{Im} \left[\frac{-1}{\varepsilon_{nl}(k, \omega)} \right] = \frac{3}{R_{WS}^3} \int_0^{R_{WS}} \text{Im} \left[\frac{-1}{\varepsilon[k, \omega, \rho_{nl}(r)]} \right] r^2 dr, \quad (2)$$

with R_{WS} the atomic Wigner-Seitz radius and $\varepsilon[k, \omega, \rho_{nl}(r)]$ the Lindhard dielectric function. The stopping power due to the interaction of the ion with the nl shell of target electrons is given by

$$S_{nl} = \frac{2Z_P^2}{\pi v^2} \int_0^\infty \frac{dk}{k} \int_0^{kv} \omega \text{Im} \left[\frac{-1}{\varepsilon_{nl}(k, \omega)} \right] d\omega, \quad (3)$$

and total stopping is the addition of FEG and inner-shell contributions $S^{\text{SLPA}} = S_{\text{FEG}} + \sum S_{nl}$.

We want to emphasize two main differences between the SLPA as given in Eqs. (2) and (3) and the usual LPA, as employed by Chu and co-workers [16], or Wang and Ma [19], among others. First, the independent-shell approach is expressed in Eq. (2) as a dielectric response that depends on the electron density of the particular shell considered, and not on the total density of electrons. Second, the original LPA formulation [11,12,14] and the subsequent extensions to intermediate energies [18,31–37], weight the spatial average of Eq. (2) with the density of electrons $\rho_{nl}(r)$. On the contrary, the present SLPA given by Eq. (2) is a simple unweighted space average.

The SLPA description of the induced potential has already been applied to the calculation of the different energy moments in a simple and consistent way, giving very good results for total stopping power or straggling of bare ions in solids [22,25] and gases [21]. Moreover, the shell-wise approach allows us to obtain ionization cross sections for each shell of target electrons, with very good agreement with the available experimental data [21–24].

For dressed projectiles, the screening stopping power S^{scr} is calculated from Eq. (1) by replacing the projectile nucleus charge Z_P by a screened one $Z_P^{\text{scr}}(k) = Z_P - Z_e(k)$, which depends on the transferred momentum k . The term

$$Z_e(k) = \sum_{n=1}^N \langle \varphi_n | e^{i\vec{k} \cdot \vec{r}} | \varphi_n \rangle \quad (4)$$

is the form factor of the N bound electrons remaining frozen in the shells. The screening stopping power is therefore expressed as

$$S^{\text{scr}} = \frac{2}{\pi v^2} \int_0^\infty \frac{dk}{k} |Z_P^{\text{scr}}(k)|^2 \int_0^{kv} \omega \text{Im} \left[-\frac{1}{\varepsilon(k, \omega)} \right] d\omega. \quad (5)$$

The antiscreening stopping power S^{antis} is calculated following Ref. [21]. It considers the energy loss when both the target and projectile electrons are excited or lost. The transition of the projectile electron from the ground state φ_i to a final state φ_f (bound or not) is described through the corresponding form factor $F_{if}(k) = \langle \varphi_f | e^{i\vec{k} \cdot \vec{r}} | \varphi_i \rangle$. The antiscreening stopping power of dressed projectiles is given by

$$S^{\text{antis}} = \frac{2}{\pi v^2} \sum_f \int_{k_{\min}}^\infty \frac{dk}{k} |F_{if}(k)|^2 \int_0^{kv-\Delta\epsilon} \omega \text{Im} \left[-\frac{1}{\varepsilon(k, \omega)} \right] d\omega, \quad (6)$$

where $k_{\min} = \Delta\epsilon/v$, with $\Delta\epsilon$ the energy gained by the projectile electron. The addition \sum_f includes the excited bound states (projectile excitation) and the continuum (projectile electron loss) [21]. In the latter, an integration in the energy of the ionized electron is required. Analogous to the bare ion case, for dressed projectiles we obtain total screening and antiscreening stopping power as the addition of inner-shell and FEG electron contributions.

In order to evaluate the importance of the antiscreening contribution we consider two collisional systems He in Al and He in Zn. The stopping power of He^{2+} , He^+ , and He^0 ions are calculated separately and the stopping power of He is obtained taking into account the ion equilibrium charge fraction q_i inside the solid [38] as

$$S^{\text{He}} = q_0 S^{\text{He}^0} + q_1 S^{\text{He}^+} + q_2 S^{\text{He}^{2+}}. \quad (7)$$

We employ the values of q_i given by the empirical fitting of Schiwietz and Grande [39,40]. This approach implies the assumption that the equilibrium charge state of the ion inside the solid is close to the measured emerging charge state.

For the bare ions He^{2+} , the stopping power is obtained from Eq. (1). For He^+ and He^0 ions we add the screening and antiscreening stopping powers of Eqs. (5) and (6).

In both targets, Al and Zn, we use the r_s value inferred from plasma frequency measurements, that is, $r_s = 2.02$ [41], corresponding to three electrons per atom in the FEG. For Al, these are the three valence band electrons, while for Zn, the experimental plasmon energy of 17 eV indicates a contribution of one electron from the $3d$ shell to the valence band [25]. The space-dependent densities $\rho_{nl}(r)$ for each shell of Al ($1s^2, 2s^2, 2p^6$) and Zn ($1s^2, \dots, 3d^9$) are obtained from the atomic Hartree-Fock wave functions [42].

The screening stopping power for He in Zn is plotted in Fig. 1 as a function of the ion impact energy. We can observe shell to shell contributions for He^{2+} , He^+ , and He^0 . It can be noted that in the stopping of He^{2+} , the FEG gives the main contribution. Moreover, the maximum of the total stopping is very close to that of the FEG. For He^+ and He^0 , the relative importance of the FEG and the inner-shell contributions changes. This explains the shift in the stopping maximum for the different ion charge states.

The antiscreening stopping power for He^0 and He^+ in Al is displayed in Fig. 2, showing projectile excitation and loss in each case. The main contribution to the antiscreening stopping power comes from the electron loss of He^0 , as expected since He^0 has two electrons and more weakly bound than the one in He^+ .

Figures 3 and 4 show the comparison of the antiscreening stopping power (projectile excitation plus loss) with the total one, and with the experimental data for He+Al and He+Zn, respectively. These figures summarize the main contribution of this work. In Figs. 3(a) and 4(a), we display the antiscreening stopping cross section of He^0 and He^+ . These values are not so low, about 10% of the total stopping maxi-

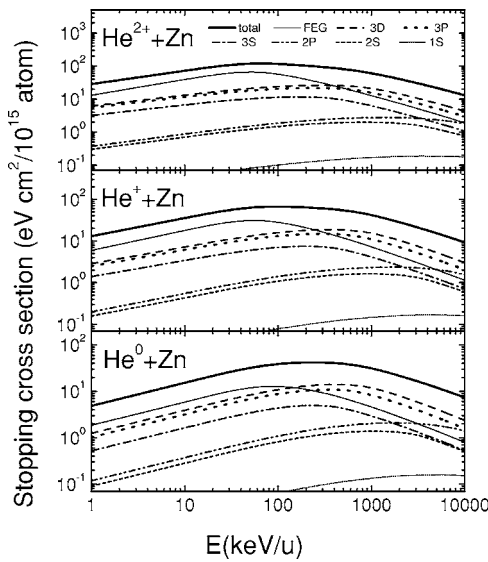


FIG. 1. Stopping power for He in Zn considering frozen ion, as a function of the impact energy. The contributions due to the FEG and the different inner shells are displayed separately.

mum, especially for energies above 200 keV. Nevertheless, when we take into account the energy-dependent fraction of He^0 and He^+ inside the solid, the antiscreening contribution falls down drastically. The equilibrium charge states q_i employed [39] are plotted in Figs. 3(b) and 4(b) to emphasize this point. Finally, Figs. 3(c) and 4(c) display the comparison between antiscreening and total stopping. The curves corresponding to projectile excitation and electron loss are obtained as the product of the antiscreening stopping power of He^0 and He^+ , and their charge fractions. These curves show that the antiscreening stopping power is very small as compared with the total one.

Present total stopping power calculations show very good agreement with the experimental data. For He in Zn, we follow a recently published work of Lantschner *et al.* [25], adding the antiscreening contribution to its results. For energies below 40 keV, the FEG nonlinear results of the ex-

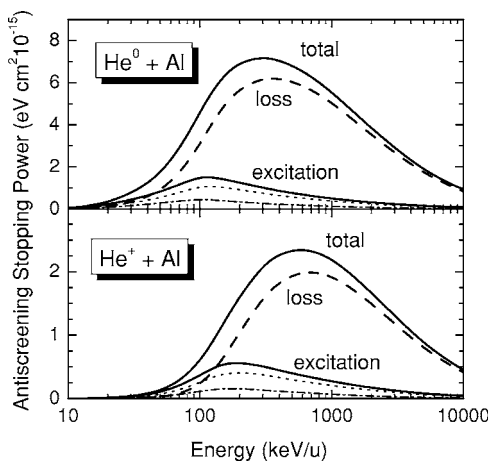


FIG. 2. Antiscreening stopping power of He^0 and He^+ in Al as a function of the energy. The contributions due to projectile electron excitation and loss are displayed separately.

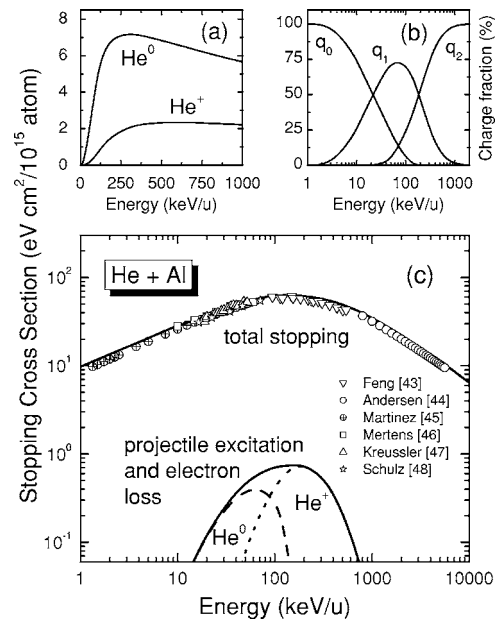


FIG. 3. (a) Antiscreening stopping power of He^+ and He^0 in Al, obtained as addition of the contributions of projectile electron excitation and loss. (b) Charge fractions of He in Al as a function of the energy [39,40]. (c) Total and antiscreening stopping power. The symbols represent the experimental data and the curves are present theoretical calculations [43–48].

tended Friedel sum rule-transport cross section by Lifschitz and Arista [8,9] are employed. At low energies, the energy loss due to the FEG employing the dielectric formalism underestimate the data, while for high energies both perturbative and nonperturbative calculations, converge [25]. An alternative to include the nonlinear effects (all orders in Z_p) within the dielectric formalism is given by the Coulomb Lindhard approximation [49], which replaces the undistorted

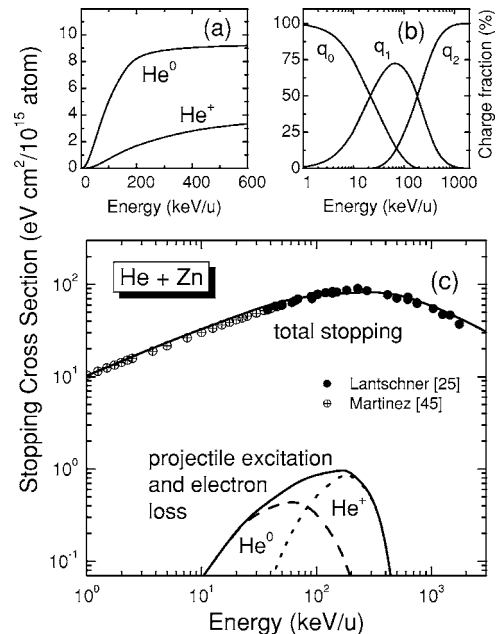


FIG. 4. The same as Fig. 3 for He in Zn.

plane waves leading to the Lindhard dielectric response, by Coulomb waves with an effective charge.

In this work we presented a theoretical description of the electronic stopping power, including the excitation and loss of projectile electrons. We used the dielectric formalism and a shell-wise local plasma approximation (SLPA) to obtain the inner-shell electron contribution. The stopping power obtained was compared with the experimental data available in the literature for He in Al and Zn. The employment of the nonperturbative results for energies below 40 keV, and the dielectric formalism for higher energies, gives a good

description of the experimental data in the range 1–6000 keV/ u . Though these results include the contribution from the excitation and loss of projectile electrons, we find that, in the case of helium ions, this contribution is only about 1% of the total stopping data, and may be neglected.

The authors want to thank N. R. Arista for his clear and detailed comments. This work was partially supported by the Argentinian Agencia Nacional de Promoción Científica y Tecnológica (Project No. PICTR-00437) and the Universidad de Buenos Aires (Project No. UBACyT X259).

-
- [1] N. Bohr, *Philos. Mag.* **25**, 10 (1913).
 [2] H. Bethe, *Ann. Phys.* **5**, 324 (1930).
 [3] F. Bloch, *Ann. Phys.* **16**, 285 (1933).
 [4] J. Lindhard, *K. Dan. Vidensk. Selsk. Mat. Fys. Medd.* **28**, 8 (1954).
 [5] P. Sigmund and A. Schinner, *Eur. Phys. J. D* **12**, 425 (2000).
 [6] P. L. Grande and G. Schiwietz, *Phys. Rev. A* **58**, 3796 (1998).
 [7] G. Maynard, G. Zwicknagel, C. Deutsch, and K. Katsonic, *Phys. Rev. A* **63**, 052903 (2001).
 [8] A. F. Lifschitz and N. R. Arista, *Phys. Rev. A* **58**, 2168 (1998).
 [9] N. R. Arista, *Nucl. Instrum. Methods Phys. Res. B* **195**, 91 (2002).
 [10] P. Sigmund and A. Schinner, *Nucl. Instrum. Methods Phys. Res. B* **195**, 64 (2002).
 [11] J. Lindhard and M. Scharff, *K. Dan. Vidensk. Selsk. Mat. Fys. Medd.* **27**, 15 (1953).
 [12] J. Lindhard and A. Winther, *K. Dan. Vidensk. Selsk. Mat. Fys. Medd.* **34**, 4 (1964).
 [13] R. H. Ritchie, *Phys. Rev.* **114**, 644 (1959).
 [14] E. Bonderup, *K. Dan. Vidensk. Selsk. Mat. Fys. Medd.* **35**, 17 (1967).
 [15] P. M. Echenique, F. Flores, and R. H. Ritchie, *Solid State Phys.* **43**, 229 (1990).
 [16] C. C. Rousseau, W. K. Chu, and D. Powers, *Phys. Rev. A* **4**, 1066 (1970).
 [17] J. F. Ziegler, *Helium Stopping Powers and Ranges in All Elemental Matter* (Pergamon, New York, 1977).
 [18] W. K. Chu and D. Powers, *Phys. Lett.* **40A**, 23 (1972).
 [19] Y-N. Wang and T-C. Ma, *Phys. Rev. A* **50**, 3192 (1994).
 [20] J. D. Fuhr, V. H. Ponce, F. J. García de Abajo, and P. M. Echenique, *Phys. Rev. B* **57**, 9329 (1998).
 [21] C. C. Montanari, J. E. Miraglia, and N. R. Arista, *Phys. Rev. A* **67**, 062702 (2003).
 [22] C. C. Montanari, J. E. Miraglia, and N. R. Arista, *Phys. Rev. A* **66**, 042902 (2002).
 [23] U. Kadhane, C. C. Montanari, and L. C. Tribedi, *Phys. Rev. A* **67**, 032703 (2003).
 [24] U. Kadhane, C. C. Montanari, and L. C. Tribedi, *J. Phys. B* **36**, 3043 (2003).
 [25] G. H. Lantschner *et al.*, *Phys. Rev. A* **69**, 062903 (2004).
 [26] E. C. Montenegro and W. E. Meyerhof, *Phys. Rev. A* **43**, 2289 (1991).
 [27] J. Neufeld and R. H. Ritchie, *Phys. Rev.* **98**, 1632 (1955); **99**, 1125 (1955).
 [28] N. Bohr, *K. Dan. Vidensk. Selsk. Mat. Fys. Medd.* **24**, 19 (1948).
 [29] P. M. Echenique, R. H. Ritchie, and W. Brandt, *Phys. Rev. B* **20**, 2567 (1979).
 [30] N. D. Mermin, *Phys. Rev. B* **1**, 2362 (1970).
 [31] C. M. Kwei, T. L. Lin, and C. J. Tung, *J. Phys. B* **21**, 2901 (1988).
 [32] C. J. Tung, R. L. Shyu, and C. M. Kwei, *J. Phys. D* **21**, 1125 (1988).
 [33] D. E. Meltzer, J. R. Sabin, and S. B. Trickey, *Phys. Rev. A* **41**, 220 (1990).
 [34] Y. F. Chen, C. M. Kwei, and C. J. Tung, *J. Phys. B* **26**, 1071 (1993).
 [35] J. Wang, R. J. Mathar, S. B. Trickey, and J. R. Sabin, *J. Phys.: Condens. Matter* **11**, 3973 (1999).
 [36] I. Gertner, M. Meron, and B. Rosner, *Phys. Rev. A* **21**, 1191 (1980).
 [37] J. F. Ziegler, *J. Appl. Phys.* **85**, 1249 (1999).
 [38] A. Arnau *et al.*, *Phys. Rev. Lett.* **65**, 1024 (1990).
 [39] P. L. Grande and G. Schiwietz, *Convolution Approximation for Swift Particles*, CasP version 3.0 (2004), code available from www.hmi.de/people/schiwietz/casp.html
 [40] G. Schiwietz and P. L. Grande, *Nucl. Instrum. Methods Phys. Res. B* **175–177**, 125 (2001).
 [41] D. Isaacson (unpublished).
 [42] E. Clementi and C. Roetti, *At. Data Nucl. Data Tables* **14**, 177 (1974).
 [43] J. S.-Y. Feng, *J. Appl. Phys.* **46**, 444 (1975).
 [44] H. H. Andersen, J. F. Bak, H. Knudsen, and B. R. Nielsen, *Phys. Rev. A* **16**, 1929 (1977).
 [45] G. Martinez-Tamayo, J. C. Eckardt, G. H. Lantschner, and N. R. Arista, *Phys. Rev. A* **54**, 3131 (1996).
 [46] P. Mertens and Th. Kirst, *Nucl. Instrum. Methods* **168**, 33 (1980).
 [47] S. Kreussler, C. Varelas, and R. Sizmann, *Phys. Rev. B* **26**, 6099 (1982).
 [48] F. Schulz and W. Brandt, *Phys. Rev. B* **26**, 4864 (1982).
 [49] J. E. Miraglia, *Phys. Rev. A* **68**, 022904 (2003).